COBEM UBERLÂNDIA 2019

ABCM Associação Brasileira de Engenharia e Ciências Mecânicas

25th ABCM International Congress of Mechanical Engineering
October 20-25, 2019, Uberlândia, MG, Brazil

A GUIDELINE TO A PRELIMINARY PROJECT OF AN AXIAL FAN USING COMPUTATIONAL FLUID DYNAMICS (CFD)

Francisco de Sousa Júnior
Douglas Melo dos Santos
Instituto Federal de Minas Gerais Campus Avançado - Av. Juscelino Kubitscheck, 485 - Distrito Industrial II, Arcos - MG
francisco.sousa@ifmg.edu.br
douglasdm9@outlook.com

Abstract.
This work presents a preliminary project guideline of an axial fan flow using a programming platform and Computational Fluid Dynamics (CFD) to get a 3D CAD model with the main geometric and aerodynamics parameters evaluated. The linear grid and lift wing theories, the radial equilibrium and the free vortex conditions were applied in this work. The guideline turned out to be very efficient, because the axial fan sizing involves a reasonable number of variables that should be admitted, calculated and after revalidate. The initially obtained results showed to be promising. However, there was a difference in the final static pressure calculated and the one pre-established in the beginning of the project. Such fact is due to the assumption of some design variables, the choice of solidity ratio and the number of calculated blades. Such difference could be minimized through the use of optimization algorithms, however this tool was not in the scope of this work. It's concluded that, even with this difference, the use of the proposed guideline is fundamental to obtain the first data to implement a more robust project of an axial fan.

Keywords: *Axial fan flow, computational fluid dynamics, aerodynamic profile.*

1. INTRODUCTION

The design of an axial fan runs into the complexity that involves several areas of mechanical engineering. The question: "Where does the project start from ?" becomes the first problem. Several variables must be admitted at the beginning of the project and then validated for consolidation. Such complexity is gradual and rise up as we walk to the final step. Thus, the definition of a basic guide to start a project becomes applicable so that the doubts are mitigated throughout the process.

The wide use of axial fans in air circulation and heat transfer process has resulted in several detailed researches aiming in increased its efficiency. Numerical investigations have been performing to quantify the efficiency of axial fans and the properties of its working fluid (Kumawat, 2014). A brief bibliography review is made in the following based on the most recent works about axial fans design, which are the basis for this project.

(Prachar, 2016) used a CFD software called "Edge" to validate the experimental data collected from a test bench built specifically for axial fans. The software is a solver that considers the fluid compressible in unstructured mesh with arbitrary elements. The Euler and Navier-Stokes equations are solved in two or three dimensions based on the finite elements method with centralized nodes. The experimental and calculated data were compared obtaining acceptable approximations between them.

(Camacho *et al.*, 2016) applied the lift wing theory and the free vortex condition in the development of a methodology for axial fans design. The rotor geometry was created using a script edited with TCL/Tk commands for the interpretation of the ICEM program. The Fluent CFD code was used to calculate the flow properties. The efficiency was calculated as a function of the mass flow considering a nominal rotation of $1770\,rpm$. The local pressure values calculated by the methodology showed minimum values of the boundary layer separation, thus increasing the equipment efficiency.

(Dwivedi and Dandotiya, 2013) investigated working fluid behavior in two types of axial fans (forward and backward skewed blade profile) using the software Fluent CFD 6.3 . The CFD analysis was performed modeling the fans using the software GAMBIT 2.2 with the $k-\epsilon$ turbulence model. The results showed a good agreement with the experimental results obtained in the literature.

The theory of fluid flow in linear grids is widely used in the aerodynamic design of turbomachinery axial rotors. As of 1940, the calculations began to incorporate some elements related to the " lift wing theory", developed specifically for aircraft wing profiles. Although this theory was developed for the study of an isolated blade (wing of an airplane), it was satisfactorily applied in axial turbomachinery with a reduced number of blades, as in pumps, fans and turbines (Camacho *et al.*, 2016).

Along with the radial equilibrium and the free vortex conditions are the most suitable and currently the most modern method in the axial fan projects. Along with the CFD reduce drastically the problems that at first, could only be diagnosed after the construction of models/prototypes. Tests in scale models or even prototypes are extremely important in the manufacturing of axial flow fans, however, a refined project will give just small adjusts in the final model, reducing the economics impacts. This theories and conditions along with CFD are applied in this work in order to structure/standardize the preliminary project of an axial fan, getting a 3D CAD model with the main global and aerodynamics parameters calculated.

2. METHODOLOGY

The linear grid and lift wing theory can be explained by Fig.(1) that shows details of the representative linear grid of the flow in an axial rotor and stator, next to its velocity triangles. The grid is composed of identical and equally spaced aerodynamics profiles, in which the spacing between the profiles is the pitch (t) and the chord length is (l). In the triangle, the absolute (C), relative (ω) and tangential (u) velocities have subscripts referring to the inlet (3), outlet (6), meridional projection (m), tangential projection (u) and referring to the medium triangle (∞). The flow angles (α) and (β) are also represented. It is also assumed that the flow proceeds on these cylindrical surfaces, without a radial component, and can be studied in the correspondent linear grid. It is also admitted a bidimensional, permanent, incompressible and not viscous (potential) flow.

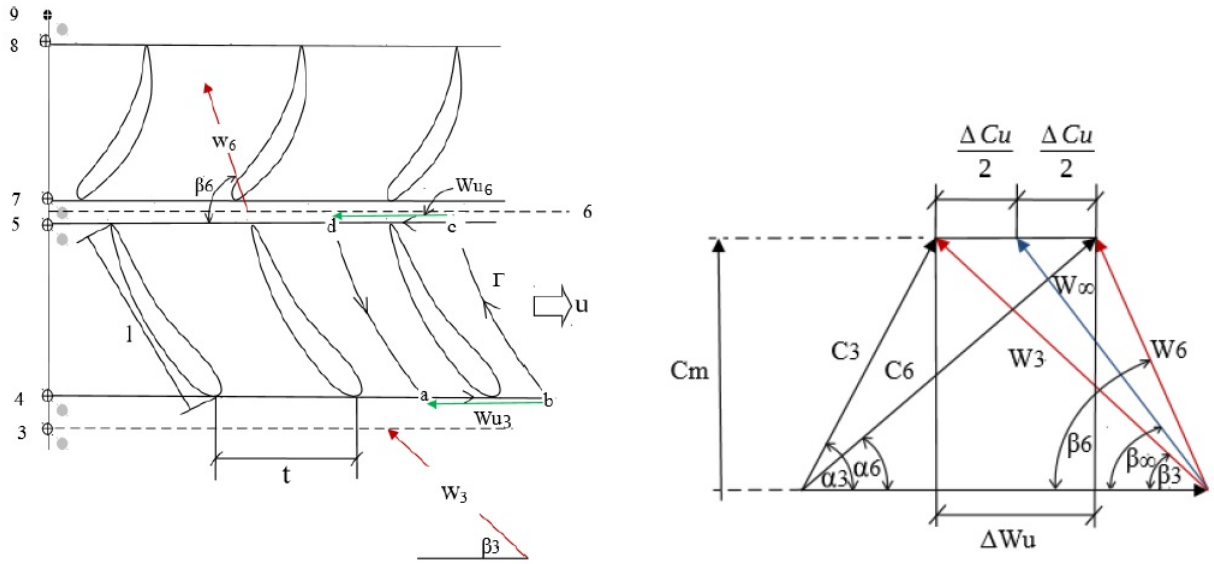

Figure 1. Mobile linear grid of an axial turbomachinery and the velocity triangles

Considering the circulation on the grid, the blade force and the lift coefficient (C_s) it can be obtained an expression that correlates the grid variables and the lift coefficient Eq. (1), where ΔC_u and ω_∞ (m/s) are the tangential component of the absolute velocity and the average relative velocity respectively.

$$C_S \frac{l}{t} = \frac{2\,\Delta C_u}{\omega_\infty} \tag{1}$$

Equation (1) composes the calculation basis of axial turbomachinery, by the lift wing theory and shows the relation between the values obtained from the velocity triangles with the dimensionless features desired for the grid profiles (Camacho *et al.*, 2013).

2.1 Radial equilibrium equation and free vortex condition

The radial equilibrium equation perform a fundamental role in the establishment of the velocity distributions (Sarmiento, 2013). In axial turbomachinery, for the axial velocity distributions in the radial direction, it can be solved by the free vortex condition and also by the forced vortex condition. In this project, the free vortex condition was used, common formulation in the hydro or aerodynamic project of axial turbomachinery, Eq. (2), where C_m and C_a (m/s) are the meridional and axial components of absolute velocity and Y_{blade} (J/kg) the specific work of the fan.

$$C_m = C_a = \text{constant} \Longleftrightarrow Y_{\text{blade}} = \text{constant} \tag{2}$$

Equation (2) reports that if $Cm = Ca$ are constants throughout the blade length, then, Y_{blade} is also constant throughout the blade length and vice versa. The free vortex condition allows axial fan projects with minimal losses, where the specific energy is is evenly distributed throughout the blade height, allowing an additional gain in operation efficiency (Camacho *et al.*, 2013).

3. GUIDELINE PROJECT

The methodology presented by (Bran and Souza, 1969) and design parameters of a rotor supplied by (Camacho *et al.*, 2013) were used to conduct the project procedure. The parameters of the axial fan under study are showed in Table 1 and also the preliminary calculations required to project the fan.

Table 1. Axial fan design parameters

Design Parameters			Preliminary Calculation		
Flow	$Q\ (m^3/s)$	2.28	Specific work	$Y\ (J/kg)$	593.5
Static pressure variation	$\Delta_{pt}\ (Pa)$	711	Shaft Power	$P_e\ (kW)$	2.165
Rotation	$n\ (rps)$	47.5	Specific rotation	$n_{qA}\ (-)$	596.5
Air density	$\rho\ (kg/m^3)$	1.2	Di/De relation	$D_i/D_e\ (-)$	0.5
Blade number	$N_{pa}\ (-)$	9	Diameter coefficient	$\delta\ (-)$	1.5
Hydraulic efficiency	$\eta\ (\%)$	80	Lightness coefficient	$\sigma\ (-)$	1.26
Outer diameter	$D_e\ (mm)$	460			
Inner diameter	$D_i\ (mm)$	230			

3.1 Axial fan preliminary design

In sequence is showed the steps for axial turbomachinery design proposed by (Bran and Souza, 1969).

1. Diameters D_i e D_e: the inner D_i and outer D_e diameters were also given as $230\,mm$ and $460\,mm$ respectively, according to the ratio $D_i/D_e = 0.5$, Table 1. Although already provided, they are verified in Cordier diagrams, through whom optimized dimensionless features are utilized to verify if the diameters are appropriate with the recommended range (Sarmiento, 2013). In addition to the hub and rotor shroud, at least two more radial stations are chosen to determine the geometry of the blade.

2. Velocity triangles: for each radial station the components of the velocity triangles are determined, Figure 1, namely:

   - The circumferential velocity (u).
   - The component of the absolute velocity in the circumferential direction (ΔC_u).
   - The average relative velocity (ω_∞).
   - The angle of the absolute flow at the outlet (α_6).
   - The angle between the tangential velocity and the average relative velocity (β_∞).
   - The product between the lift coefficient and the solidity ratio $(C_s(l/t))$. According to Eq. (1), this product is determined from the calculated values of the velocity triangles

3. Pitch (t): the distance between each blade in each radial station is calculated.

4. Solidity ratio (l/t): a fundamental geometric parameter is the solidity ratio (l/t). The chosen values depend on the designer's experience, because so far no general and consistent rule was formulated for its choice (Resmini, 2013). Two correlations published about the effect of the solidity ratio were tested. The first presented by (McKenzie, 1997), based on the Rolls Royce Aero Division studies suggests a linear relation between the inverse of the solidity ratio (t/l) and the pressure coefficient (C_{pi}), Eq. (3) e Eq. (4):

$$\frac{t}{l} = 9 \cdot (0.567 - C_{pi}) \tag{3}$$

$$Cpi = 1 - (\omega_6/\omega_3)^2 = 1 - \left(\frac{cos(\pi/2 - tan^{-1}(C_m/u))}{cos(\pi/2 - tan^{-1}(C_m/(u - \Delta C_u)))} \right)^2 \tag{4}$$

The second correlation published by (Howell, 1942) is a result of a theoretical and experimental work that showed for the first time that the tangential deflection depends only on the solidity ratio, for a wide range of outlet conditions, Eq. (5):

$$tan((\pi/2 - \beta_3)) - tan((\pi/2 - \beta_6)) = \frac{1.55}{1 + 1.5 \cdot (t/l)} \tag{5}$$

Besides the correlations cited, two criteria were still studied for the preliminary project, namely: the *De Haller* number, defined as a ratio between the relative velocities of the flow (ω_6/ω_3) and the diffusion factor (D_f), Eq. (6), that is defined as a loading parameter of the blade for an incompressible and bidimensional fluid flow (McKenzie, 1997). In Eq. (6) $\alpha_1 = (\pi/2 - tan^{-1}(C_m/u))$ and $\alpha_2 = (\pi/2 - tan^{-1}(C_m/(u - \Delta C_u)))$.

$$D_F = (1 - cos\,\alpha_1/cos\,\alpha_2) + 0.5 \cdot (t/l) \cdot cos\,(\alpha_1 \cdot (tan\,\alpha_1 - tan\,\alpha_2) \tag{6}$$

5. Lift coefficient (C_s): having the solidity ratio and the components of the velocity triangles, the lift coefficient is calculated.

6. Profile chord (l): having the solidity ratio and the pitch, the chord length of the blade profile is calculated in each radial station.

7. Aerodynamic profile: using the polar diagram that relates the lift coefficient (C_s) and the drag coefficient C_a, Figure 2, is chosen the profile that the slip coefficient is the minimum ϵ_{min}, given that $tan(\epsilon) = (Ca/Cs)$.

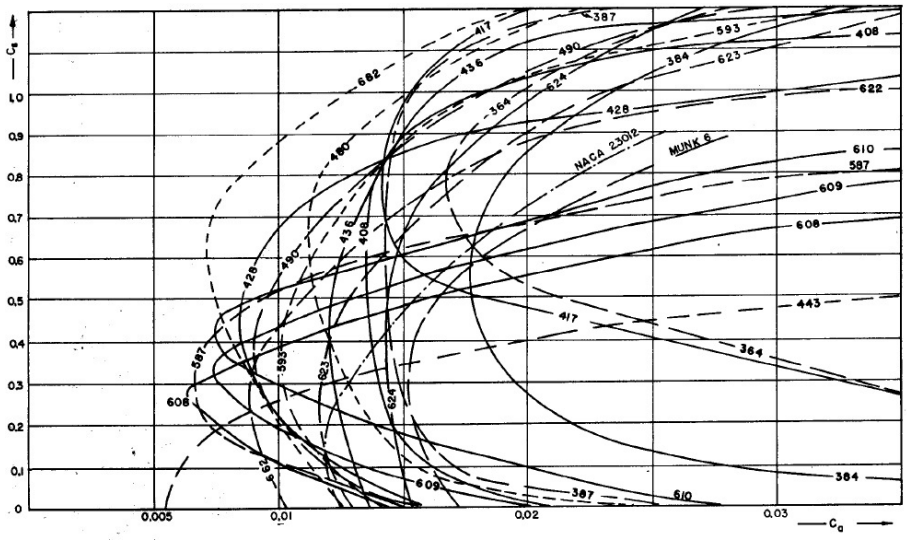

Figure 2. Polar curves CA X CS (Bran and Souza, 1969)

8. Maximum profiles thicknesses (y_{max}): due the requirements of mechanics of materials, the maximum profiles thicknesses are estimated. This evaluation can be consider a combined effect of stresses: normal stresses due to the bending moment caused by the lift forces and normal stress due to the centripetal force on the rotating blades (Camacho *et al.*, 2013). The maximum thicknesses can be approximated by Eq. (7), where a and b are constants available for the family of aerodynamic profiles chosen. The relative thicknesses (y_{max}/l), ratio between the maximum profile thickness and the chord length of each radial station is also calculated.

$$C_s = a\frac{y_{max}}{l} + b\delta \tag{7}$$

9. After choosing the profiles, the angle of attack (δ) and the angle of blade assembly (β) are calculated. The angle of attack must decrease smoothly from the hub to the blade tip, avoiding negative or very large values (close to the stall of the profile). Figure 3 shows the angles δ e β in a cylindrical cut in a radial station.

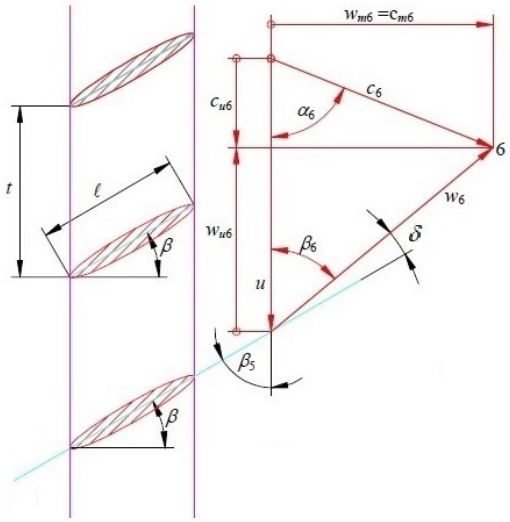

Figure 3. Angles δ e β (Sarmiento, 2013)

10. Tuning coefficient C_0: the ratio between the maximum profile thickness in the radial station and the maximum thickness of the base profile $(y_{max}/l/(y_{max/l})_b)$ is calculated. The maximum thickness of the base profile is known for each profile family.

11. Reynolds number: the Reynolds number is calculated based on the chord length of the aerodynamic profile, Eq. (8).

$$R_e = \frac{\rho \cdot \omega_\infty \cdot l}{\mu} \tag{8}$$

12. Slip coefficient (ϵ): used as a criteria for choosing blade profiles, it is calculated by $\epsilon = arctg(C_a/C_s)$.

13. Degree of reaction τ: calculated based on the velocity triangles, the range of values are between 0 and 1, where $\tau = 0$ characterizes an action machine and $\tau > 0$ a reaction machine.

3.2 CFD Guideline

After the axial fan preliminary design, the project follows to the numerical simulation, which is composed of three parts: Pre-processing, solver and post-processing, showed in the flowchart below:

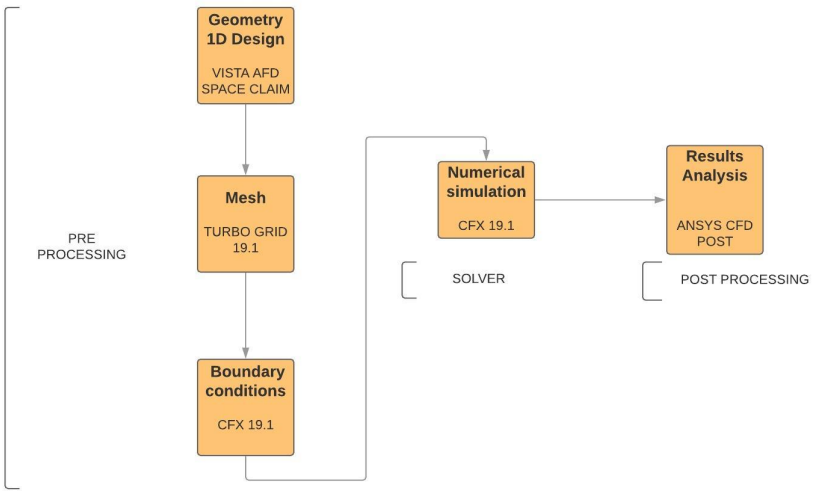

Figure 4. Processing steps

The simulation steps are described in the following:

1. 1D design and geometry generation: a preliminary analysis of the axial fan performance is done from the operating and geometric parameters initially calculated. The VISTA AFD®, a tool of the ANSYS WORKBENCH® for turbomachinery design was used. This software generates the preliminary design in 1D and a fan performance estimate. The blade geometry is created from the data imported from the VISTA AFD® into the DESIGN MODELER®, a 3D modeling software.

2. Mesh: to generate the mesh the TURBO GRID 19.1® was used for the creation of a periodic channel for one fan blade. The simulation in a channel with periodicity condition is applied in turbomachinery based on the radial equilibrium hypothesis, running the analysis only in one domain referring to one blade. The mesh generated has 206024 elements, Figure 5, with a region of refinement of the mesh next to the leading and trailing edges of the blade. This refinement has vital importance because the mesh quality in this regions has a great influence to obtain a reliable solution (Sarmiento, 2013).

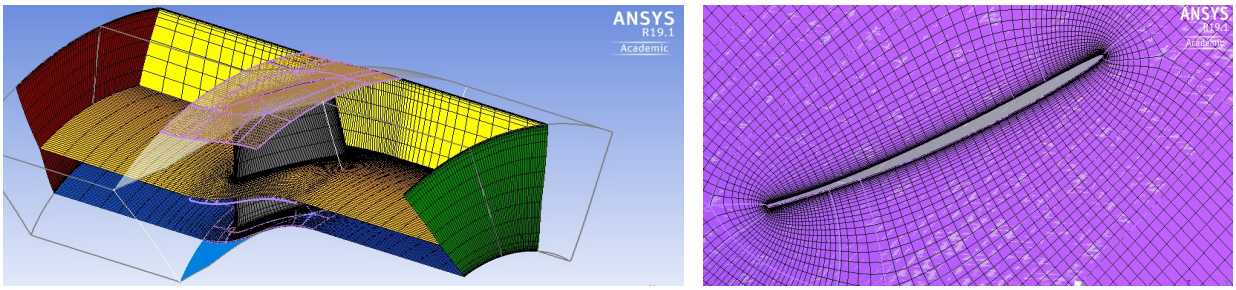

(a) Periodic channel (b) Refinement region

Figure 5. Mesh generated in the periodic channel. Images used courtesy of ANSYS, Inc.

3. Boundary conditions: the mesh generated in the computational domain was exported to CFX 19.1 ® and the boundary conditions inserted for the solution of the flow equations. The boundary conditions are defined as follow:

   - Inlet surface: in the inlet of the periodic channel a mass flow of $2.736\,kg/s$ is specified, $1/9$ of this value specified for each channel referring to one isolated blade. The working fluid is defined as air at $25°C$. The initial gauge pressure is defined as zero considering the atmospheric pressure as reference. The level of turbulence intensity is set to 5 % and turbulent viscosity rate set to 5.
   - Outlet surface: in the outlet channel is used the outflow condition. When using this condition, it is not necessary to define any characteristic property of the flow in the outlet surface, as pressure and velocity. Such condition was choice so that can be possible comparing the values obtained by the numerical simulation and the values of the preliminary project.
   - Periodic surfaces: the rotational periodicity condition is defined for the walls of the domain referring to one isolated blade which border the adjacent domain, equaling the properties with the neighboring cells of the opposite periodic plan. The rotation speed is defined as $2850\,rpm$, according to Table 1.
   - Walls: the wall boundary condition is used in the solid regions through where the fluid flows, which may be stationary or can move (Sarmiento, 2013). In the analyzed domain, the hub and the shroud were defined as walls with rotational movement ($2850\,rpm$) and also defined with the no slip condition.

4. Solver: the k-ϵ *standard* turbulence model was defined. It is commonly used as turbulence model for industrial applications due to easy convergence. It is considered a robust and a reasonably accurate model, having submodels of compressibility, thrust, combustion, multiphase, etc, (Sarmiento, 2013). It was necessary to define the convergence criteria for the interactive solution, measuring the error in the solution of the flow equation system. The convergence criteria used was the Root Mean Square (RMS), defined as $1 \cdot E^{-4}$, standard value of the Solver, enough in many applications.

4. RESULTS

The results of the preliminary design are showed in this section. The steps described in section 3.1 were executed in four radial stations, hub $(230\,mm)$, tip $(460\,mm)$ and two equidistant radial stations $a = (307\,mm)$ and $b = (383\,mm)$. The Table 2 shows the result of the step 2, referring to the components of the velocity triangles.

Table 2. Values of the velocity triangles

Station	D	u	ΔC_u	$alpha_6$	ω_∞	β_∞
-	mm	m/s	m/s	degrees	m/s	degrees
hub	230	34.32	21.60	40.2	29.79	37.88
a	307	45.81	16.18	48.5	41.92	25.87
b	383	57.15	12.97	54.6	53.86	19.85
tip	460	68.64	10.80	59.4	65.83	16.13

Having the data of the velocity triangles, the calculation follow to the next steps. In the step four, a deep study was performed to verify the suitable solidity ratio using the two criteria cited, the *De Haller* number and the diffusion factor. The values chosen for the solidity ratio in the axial fan under study (Camacho *et al.*, 2013) are very close to the values chosen by (Bran and Souza, 1969), also in the design of an axial fan with $De = 360\,mm$ and $Q = 1.0, m3/s$, as shown in Table 3.

Table 3. Solidity ratio (l/t)

Camacho *et al.* (2013)	(l/t)	Bran and Souza (1969)	(l/t)
Hub $(230\,mm)$	1.20	Hub $(180\,mm)$	1.30
a $(307\,mm)$	0.85	a $(240\,mm)$	0.85
b $(383\,mm)$	0.65	b $(300\,mm)$	0.60
Tip $(460\,mm)$	0.50	Tip $(360\,mm)$	0.43

The first correlation tested , published by (McKenzie, 1997), Eq. (3) and Eq. (4) was inconsistent due to the negative solidity ratio obtained, what is mathematically inconsistent. According to the methodology, the value of the pressure coefficient (Cpi) should not be much greater than 0.5 for good approximations. The inconsistent solidity ratio calculated is due to the Cpi calculated in the hub of 0.67. In this case, what is done according to the methodology is to change the cube ratio Di/De to obtain more suitable values, that is described in practice in the range of 0.5 to 1.5 for the inverse of the solidity ratio (t/l).

The second correlation tested published by (Howell, 1942), Eq. (5) was also not considered a good approximation due to the high value of solidity ratio found in the hub, which cause huge losses. It should be noted that even previous studies can predict about the effect of the solidity ratio throughout the project, none of them allows itself to choose the suitable solidity ratio without the support of a loss prediction model or an interactive process (Resmini, 2013), looking to the discrepancy in the comparison of the results in the two applied methods, leading to different values.

The diffusion factor for the solidity ratio used by (Camacho *et al.*, 2013) and for the values calculated by the approximation of (Howell, 1942) was calculated. For the the solidity ratio approximated by the model of (McKenzie, 1997) the diffusion factor was not calculated due to the inconsistent obtained values. The Table 4 shows the values obtained with the *De Haller* number, as the first approximation criteria for the allowed diffusion.

Table 4. Diffusion factor and *De Haller* number

$D\,(mm)$	Diffusion factor		*De Haller* number
	(Howell, 1942)	(Camacho *et al.*, 2013)	
230	0.48	0.66	0.53
307	0.38	0.49	0.70
383	0.29	0.37	0.80
460	0.23	0.30	0.85

The results in Table 4 show that for both solidity ratio, by (Camacho *et al.*, 2013) and the approximate one by (Howell model, 1942) are outside of the recommended range. Already in the first criteria, the *De Haller* number indicates that the dimensions of the rotor must be changed so that the diffusion factor can be calculated as the final criteria, following this design methodology.

With the solidity ratio determined, the lift coefficient C_s is calculated. The table 5 shows the result of the steps 3 to 13 in each radial station, already chosen the aerodynamic profiles by the polar diagram of Figure 2.

Table 5. Calculations for each radial station using the base profiles GÖ 682 e GÖ 428

Station	$C_s \cdot l/t$	l/t	t	l	C_s	Profile	y_{max}	y_{max}/l	δ	β	C_0	R_e	ϵ	τ
-	-	-	mm	mm	-	-	mm	-	graus	degrees	-	10^5	-	-
Hub	1.450	1.20	80.28	96.3	1.210	GÖ 682	9.0	0.0934	8.28	46.16	0.877	2.0	0.017	0.685
a	0.772	0.85	107.2	91.1	0.908	GÖ 682	8.0	0.0878	5.29	31.16	0.824	2.7	0.012	0.823
b	0.482	0.65	133.7	86.9	0.741	GÖ 428	7.0	0.0805	3.85	23.70	0.976	3.3	0.016	0.886
Tip	0.328	0.50	160.6	80.3	0.656	GÖ 428	6.0	0.0747	3.23	19.36	0.905	3.7	0.014	0.921

4.1 Comparison with the numerical simulation

The result of the VISTA AFD ® analysis is showed in Figure 6, with the 3D model of the axial fan. The red highlight indicates values outside of the recommended range.

(a) Preliminary result (b) Axial fan 3D model

Figure 6. *Vista Afd* ®analysis. Images used courtesy of ANSYS, Inc.

As shown in Table 4, already in the initial criteria, the *De Haller* number outside of the recommended range on the rotor hub indicates that the losses will be excessive in that region. The value of the *De Haller* number for the hub obtained was 0.47, close to 0.53 calculated in the preliminary design, Table 4, also outside of the recommended range (> 0.72). Another high parameter is the loading on the hub. In general, the rotor presents good parameters according to the calculation in the meanline, and the geometry can be altered by the solidity ratio or cube ratio as required.

In the third part of the numerical simulation, a report is generated by the CFD-Post® about the fan efficiency and flow properties based on the blade dimensions calculated in preliminary project. Figure 7 shows the variation of the total and static gauge pressures during the flow. In the x-axis, streamwise location is the position in the periodic channel, where "0" refers to the inlet and "1" to the outlet.

It can be seen that the total pressure P_t remains in $0\,Pa$, that is, equal to the reference atmospheric pressure, till it passes along the blade where the pressure is increased in $673\,Pa$. The static pressure P_s from the inlet is smaller than the atmospheric pressure due the air suction. When the flow passes through the fan, there is a gain of $574\,Pa$.

This static pressure difference P_s of $574\,Pa$ obtained in the simulation is lower than $711\,Pa$ stipulated. Consequently, with $574\,Pa$, the components of the velocity triangles differ from the initial design, which results in small differences in the assembly angle β and the blade lift coefficient C_s.

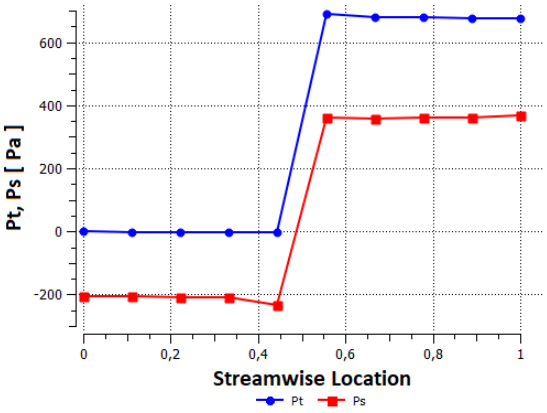

Figure 7. Variation of the static (Ps) and total (Pt) gauge pressures. Images used courtesy of ANSYS, Inc.

In the Figure 8 is showed the relative velocities streamlines along the blades. The velocities increase from the hub to the tip.

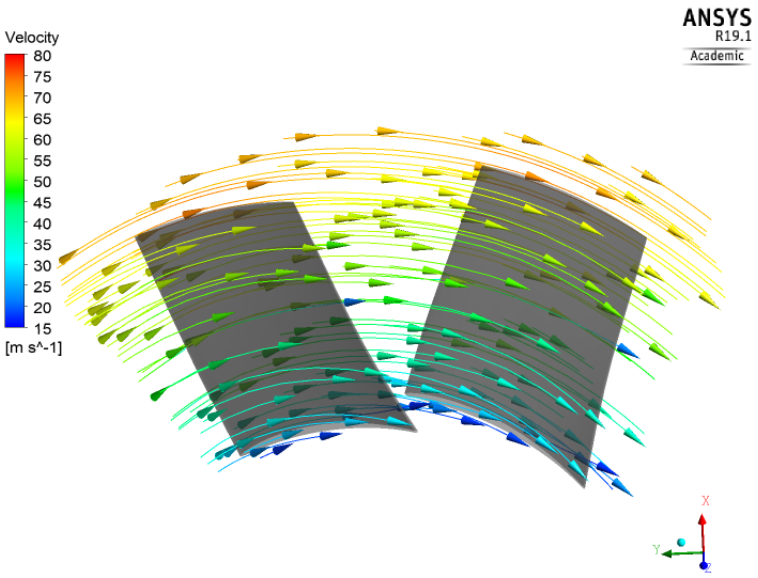

Figure 8. Relative velocities vectors. Images used courtesy of ANSYS, Inc.

5. CONCLUSION

The numerical simulation indicated a variation in static air pressure of $574Pa$, lower than $711Pa$ that was initially expected by the preliminary project. Due to this difference, the following hypotheses are discussed why the value of $711Pa$ was not achieved:

- Increased mesh refinement: the student version of ANSYS 19.1® was used, with limitations on the number of elements in the computational mesh. Although sufficient for this case, a better refinement of the mesh in a software with a professional license would lead to more accurate results.

- Inner and outer diameters of the fan: the diameters initially provided, were compared through Cordier diagrams (Bran and Souza, 1969), used to verify if the diameters are in the recommended range. According to the methodology of (Camacho *et al.*, 2013), it is reasonable use the external diameter as $460\,mm$ and hub/tip ratio as 0.50 because it is near to the values indicated by the diagrams. An alternative would be approximate more or use the diagrams values, monitoring the static pressure behavior through another numerical simulations.

- Selected solidity ratio: as reported in section 3.1, the solidity in general is chosen by the designer's experience. Other values can be tested through CFD, the diffusion factor and *De Haller* number criteria, that in the preliminary project and in the numerical simulation indicated excessive losses in the rotor hub.

- Number of blades: if it is not a design constraint, it can be tested to increase or decrease the number of fan blades and analyses if there will be any changes in the static pressure.

The parameters cited above can be changed together and tested, which would conduct to an optimization work to find the best dimensions, so that, the fan works around $711\,Pa$ of static pressure variation, as intended. Despite of the difference in the final static pressure obtained, it's concluded that, even with this difference, the use of the guideline proposed here is fundamental to obtain the first data to implement a more robust project of an axial fan.

Considering that an optimization work was not the goal of this project, one suggestion for future works would be study the variation of the geometric parameters as mentioned, a case of numerical optimization of the blade geometry.

6. ACKNOWLEDGEMENTS

The authors are grateful to IFMG for the financial support in this project.

7. REFERENCES

Bran, R. and Souza, Z., 1969. *Máquinas de fluxo: turbinas, bombas, ventiladores*. Ao Livro Tecnico.

Camacho, P.R.G.R., Filho, P.N.M., Ricci, P.J.E.R., and Albuquerque, P.M.R.B.F., 2013. "Teoria da asa de sustentação aplicada às máquinas de fluxo". *Unifei - Universidade Federal de Itajubá*.

Camacho, R.G.R., Oliveira, W.D., Santos, E.C.D., Silva, E.R.D., Angulo, T.M.A., Costa, C.E.A.D. and Reis, T.C.A.D., 2016. "Methodology of preliminary design and performance of a axial-flow fan through cfd". *International Journal of Aerospace and Mechanical Engineering*.

Dwivedi, D. and Dandotiya, D.S., 2013. "Cfd analysis of axial flow fans with skewed blades". *IJETAE*, Vol. 3, No. 10, pp. 741–752.

Howell, A., 1942. *The Present Basis of Axial Flow Compressor Design. Pt. 1. Cascade Theory and Performance*. ARC technical report. H.M. Stationery Office.

Kumawat, H., 2014. "Modeling and simulation of axial fan using cfd".

McKenzie, A., 1997. *Axial Flow Fans and Compressors: Aerodynamic Design and Performance*. Cranfield Series in Turbomachinery. Ashgate. ISBN 9780291398505.

Prachar, A., 2016. "Comparison of axial fan rotor experimental data with cfd simulation". *Acta Polytechnica*, Vol. 56, No. 1, pp. 62–66.

Resmini, M., 2013. "Numerical investigation of the solidity effect on a linear compressor cascade performance and stability". *COPEC*.

Sarmiento, A.L.E., 2013. "Desenvolvimento de uma metodologia para o projeto aerodinâmico de rotores axiais reversíveis de ventiladores de jato de túneis rodoviários". *Unifei - Universidade Federal de Itajubá*.

8. RESPONSIBILITY NOTICE

The authors are the only responsible for the printed material included in this paper.